Synthesis and characterization of aluminum doped zinc oxide nanoparticles via a novel and low cost aqueous chemical process

A. Moussa Tankari, K. Medjnoun, M. Nouiri, Olivier Briot, S. Juillaguet, H. Peyre, M. Belaqziz, Kamal Djessas

Materials Letters 353 (2023) 135230

Contents lists available at ScienceDirect

Materials Letters

journal homepage: www.elsevier.com/locate/matlet

Synthesis and characterization of aluminum doped zinc oxide nanoparticles via a novel and low cost aqueous chemical process

A. Moussa Tankari [a], K. Medjnoun [a], M. Nouiri [b], O. Briot [c], S. Juillaguet [c], H. Peyre [c], M. Belaqziz [d], K. Djessas [a,*]

[a] Laboratoire Procédés, Matériaux et Énergie Solaire CNRS UPR 8521, Université de Perpignan, Perpignan, France
[b] Laboratory of Physics of Materials and Nanomaterials Applied at Environment, Gabes University, Gabes, Tunisia
[c] Laboratoire Charles Coulomb UMR 5221, CNRS, Université de Montpellier, Montpellier, France
[d] Laboratory of Processes for Sustainable Energy & Environment, Cadi Ayyad University, Marrakesh, Morocco

ARTICLE INFO

Keywords:
Nanoparticles
Aluminum doped ZnO
Crystallographic structure
Photoluminescence

ABSTRACT

Pure and Aluminum doped Zinc Oxide Nanoparticles (AZO NPs) with various doping concentrations were synthesized using an original aqueous chemical process under atmospheric pressure and moderate temperature, using only deionized water as a solvent with a filtration step followed by heat treatment.

The X-Ray Diffraction (XRD), Raman and Field Emission Scanning Electron Microscopy- Energy-Dispersive X-ray Spectroscopy (FESEM-EDS) analysis of nanoparticles reveals a hexagonal wurtzite structure, with a size around 60 nm and the presence of aluminum in our samples. Optical investigations demonstrate that the material is of high quality, with few deep structural defects, since Photoluminescence (PL) is largely dominated by excitonic emission at low temperatures.

1. Introduction

Currently, doped Zinc Oxide Nanoparticles (ZnO NPs), have attracted considerable attention to the scientific community due to their abilities to improve electrical and optical properties of material, but also for sensing, photocatalysis, thin films and other applications [1–7]. These applications result from Zinc Oxide (ZnO) remarkable optical properties, such as a large exciton binding energy (60 meV) [8], the possibility of doping and co-doping to develop additional properties. Many techniques have been used to synthesize doped and undoped ZnO NPs, such as the precipitation method [9], the sol–gel process [10], and the hydrothermal process [11]. However, the main limitations of these chemical techniques are the use of various organic solvents and stabilizers that can be toxic. In this paper, we present an original experimental protocol based on aqueous chemical process at low temperature and atmospheric working pressure, which is environmentally friendly and allows for an easy and reproducible control of aluminum doping in the ZnO lattice.

2. Experimental

AZO NPs were synthesized by an original aqueous chemical process using only deionized water as solvent with zinc acetate dihydrate $C_4H_6O_4Zn$ ($2H_2O$) and aluminum nitrate $Al(NO_3)_3$ ($9H_2O$) as dopant. First, the precursors are dissolved in solvent under magnetic stirring at atmospheric pressure and room temperature. The solution is heated at 70 °C for 10 min, then to 150 °C until complete evaporation of the solvent. The formed xerogel ground into nanopowders. The nanoparticles were initially cleaned by dispersing them in 100 ml of ethanol using an ultrasonic bath. Subsequently, they were filtered through nylon membrane filter in a buchner funnel. This filtration process was repeated three times before the final drying step at 180 °C for 3 h.

Their structural properties were studied by X-ray diffraction (Philips X'pert, Cu-Kα radiation (λ = 0.15406 nm)). Morphological and compositional analysis was carried out using FESEM analysis (Hitachi S-4500) and EDS analysis (KEVEX Si [Li]). Raman analysis were performed using Horiba Jobin-Yvon LabRAM. Photoluminescence measurements were realized at different temperatures with a Jobin-Yvon triax 550 spectrometer.

* Corresponding author.
E-mail address: djessas@univ-perp.fr (K. Djessas).

https://doi.org/10.1016/j.matlet.2023.135230
Received 20 July 2023; Received in revised form 12 September 2023; Accepted 12 September 2023
Available online 14 September 2023

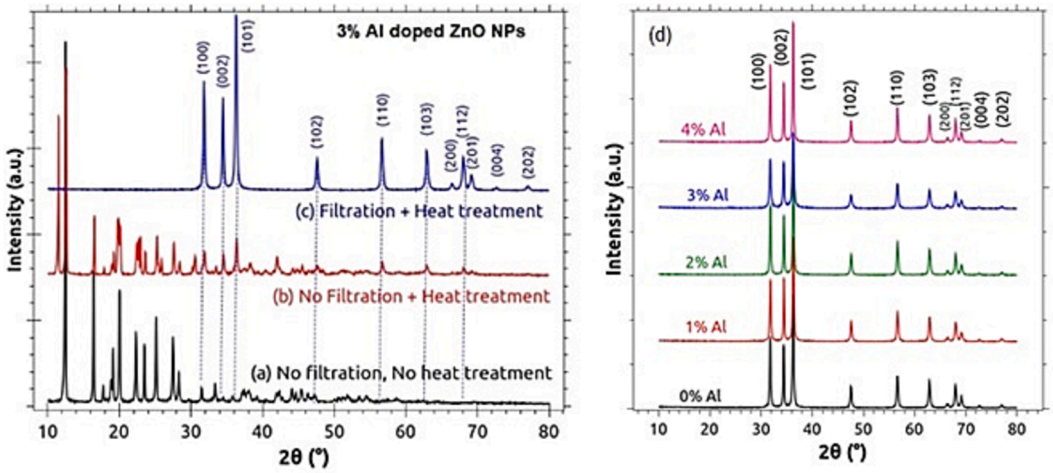

Fig. 1. XRD patterns of nanoparticles: (a) no treatments, (b) with heat treatment, (c) with filtration and heat treatment and (d) with different aluminum doping concentration.

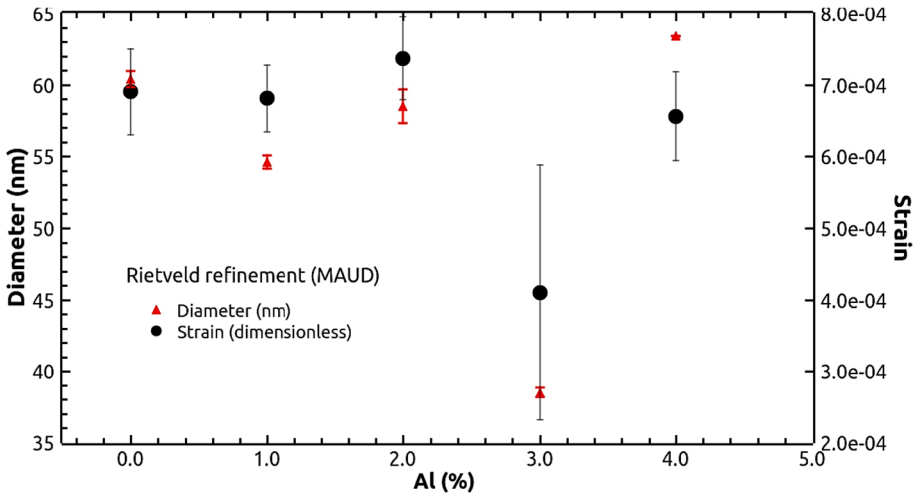

Fig. 2. Nanoparticle sizes and microstrain versus aluminum doping, extracted from Rietveld refinement.

3. Results and discussion

In order to optimize the synthesis protocol of our ZnO NPs, we have performed structural characterization at different steps of the process. The XRD patterns related to these steps are depicted in Fig. 1. The as-synthesized AZO NPs present an XRD pattern with dominated secondary phases including the ZnO peaks (Fig. 1.*a*). All these secondary phases are related to the used precursors. After the thermal treatment at 180 °C for 3 h, we have noticed the enhancement of the resolution of the peaks attributed to ZnO phase (Fig. 1.*b*). The pattern of nanoparticles after performing filtration and heat treatment at 180 °C for 3 h are shown in Fig. 1.*c*. We observed only the hexagonal wurtzite ZnO structure according to JCPDS N° 36–1451 [12] with good crystallinity.

The reproducibility of the synthesis process has been confirmed by the preparation of pure and aluminum doped ZnO nanoparticles with different concentrations (0, 1, 2, 3 and 4%) following the same protocol. Their XRD pattern are illustrated in Fig. 1.*d*.

It is noteworthy that changing the aluminum content does not lead to drastic changes in the diffraction pattern. In particular, the peak position remains unchanged for all Aluminum (Al) contents, at the precision of the experiment (a step of 0.02° was used) and owing to the noticeable widths of the peaks. The lattice parameters of the AZO nanoparticles are a = 3.246 Å and c = 5.206 Å. These values are very close to those of wurtzite ZnO. The simple approach using the Debye-Scherrer equation [13] may not be used here to analyze the linewidths, since they are evolving with the diffraction angle.

Then in our case, a more sophisticated analysis was performed, making Rietveld refinements, using the MAUD software package [14], of the x-ray diffraction patterns. Lattice parameters as well as particle sizes and strain were refined and the results are displayed in Fig. 2. The nanoparticle sizes are roughly constant, around 60 nm, and much lower strain values are deduced. This positive strain corresponds to a slight tensile deformation. This demonstrates that aluminum doping does not introduce strong structural modifications in the ZnO lattice, which can be explained by the fact that the Aluminum atom has a much lower ionic radius than Zinc, and can thus easily substitute Zinc on its crystal structure.

The size of Al (3%) doped ZnO nanoparticles shown in Fig. 3a, achieved by FESEM analysis, are in perfect agreement with the x-ray diffraction data. The sample consist of a mixture of rods and spherical shaped nanoparticles. Similar morphology for metal doped ZnO nanoparticles obtained by sol gel process under supercritical conditions was reported in our previous works [15–16]. EDS analysis were used to determine the elemental composition of the synthesized AZO NPs. EDS spectrum of Al (3%) doped ZnO nanoparticles (Fig. 3b) shows peaks for zinc (Zn), oxygen (O), and aluminum (Al) atoms, without any impurities detected. The elemental compositions values obtained for the $Zn_{1-x}Al_xO$ nanoparticles with different aluminum concentrations × ($0 \leq x \leq 0.04$)

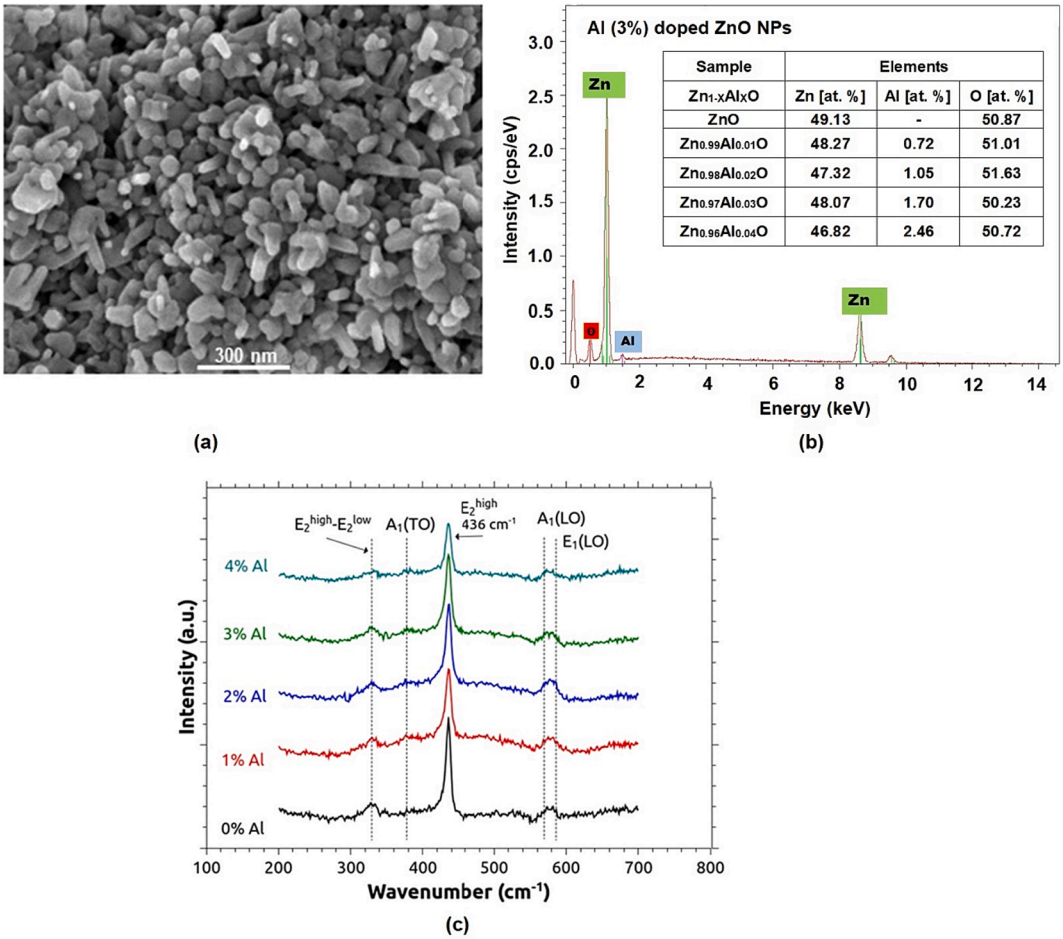

Fig. 3. $Zn_{0.97}Al_{0.03}O$ nanoparticles analysis: (a) FESEM image, (b) EDS elemental composition and (c) Raman spectra of AZO nanoparticles.

given in the insert table, are quasi-stoichiometric, affirming the purity achieved through filtration and thermal treatment.

Group theory predicts that ZnO vibration modes (Γ opt) will exhibit the following irreducible representation: $\Gamma\ opt = A_1 + E_1 + 2E_2 + 2B_1$, where B_1 modes are silent, A_1 and E_1 are polar modes (both Raman and infrared active), while E_2 modes (E_2^{low}, E_2^{high}) are nonpolar and Raman active only. The E_1 and A_1 modes which are polar modes and can be split into longitudinal (LO) and transversal optical (TO) phonons. The B_1 mode is silent and is thus not observed. The Raman spectra of pure and Al-doped ZnO nanoparticles is depicted in Fig. 3*c*. We notice the presence of peaks located at 331 cm^{-1}: $E_2^{high} - E_2^{low}$, 379 cm^{-1}: A_1(TO), 436 cm^{-1}: E_2^{high}, 569 cm^{-1}: A_1(LO) and 586 cm^{-1}: E_1(LO), in all samples. The peak located at 436 cm^{-1} is the characteristic of the hexagonal wurtzite phase of ZnO and assigned to the E_2^{high} mode [17]. It exhibits no noticeable shift with increasing Al doping. This, combined with the fact that it is redshifted by about 1 cm^{-1} from its theoretical position is in good agreement with the weak tensile strain deduced from our Rietveld refinements, taking into account phonon deformation potentials published by *Callsen et al.* [18].

Photoluminescence experiments were carried on our samples at a temperature of 20 K. First, a large scan covering both the near band edge region and the deep emission region is presented in Fig. 4*a*

In the near band edge zone, two peaks dominate. They are attributed to the exciton bound to donors (D0X) and Donor Acceptor Pair (DAP) recombination. A striking feature of this figure is that, even at the highest doping levels, deep emission bands related to structural defects are absent. This is a testimony of the high quality of the material in the whole range of doping investigated here. A more detailed view of the near band edge luminescence is presented in Fig. 4*b*.

At an energy of 3.384 eV, the free exciton is observed. This occurs at slightly lower position, by 1–2 meV than reported elsewhere [19]. This can be interpreted as an effect of the slight tensile strain experimented by our samples, as deduced from the XRD data. Similarly, the D0X bound exciton is seen at 3.348 eV, followed by the DAP line at 3.308 eV and its LO phonon replica at 3.238 eV. At increasing doping levels, the intensity ratio between the D0X and DAP lines gradually reverses, demonstrating the effective increase of doping species. Concerning the absence of deep emissions, one could question the effect of temperature, since broad band defect emissions are strongly phonon assisted processes. In order to investigate this aspect, the temperature dependent photoluminescence experiments have been carried out and the results are depicted in Fig. 4*c*. From it, we can have noticed that even at higher temperatures, up to room temperature, no deep defects PL band arises. Only a decrease in the PL intensity, along with a broadening of the near band edge features can be observed. This establishes the potential of our synthesis method, leading to a material of high quality, with a low content of structural defects..

4. Conclusion

We have presented a new synthesis method for the growth of undoped and aluminum doped nanoparticles of ZnO. This technique is extremely simple, involving an aqueous route and simple precursors, no autoclave step is required. This method is both safe and inexpensive, and may readily transfer to an industrial scale. We have demonstrated that the material produced is of high structural quality and high purity, from structural and optical characterization.

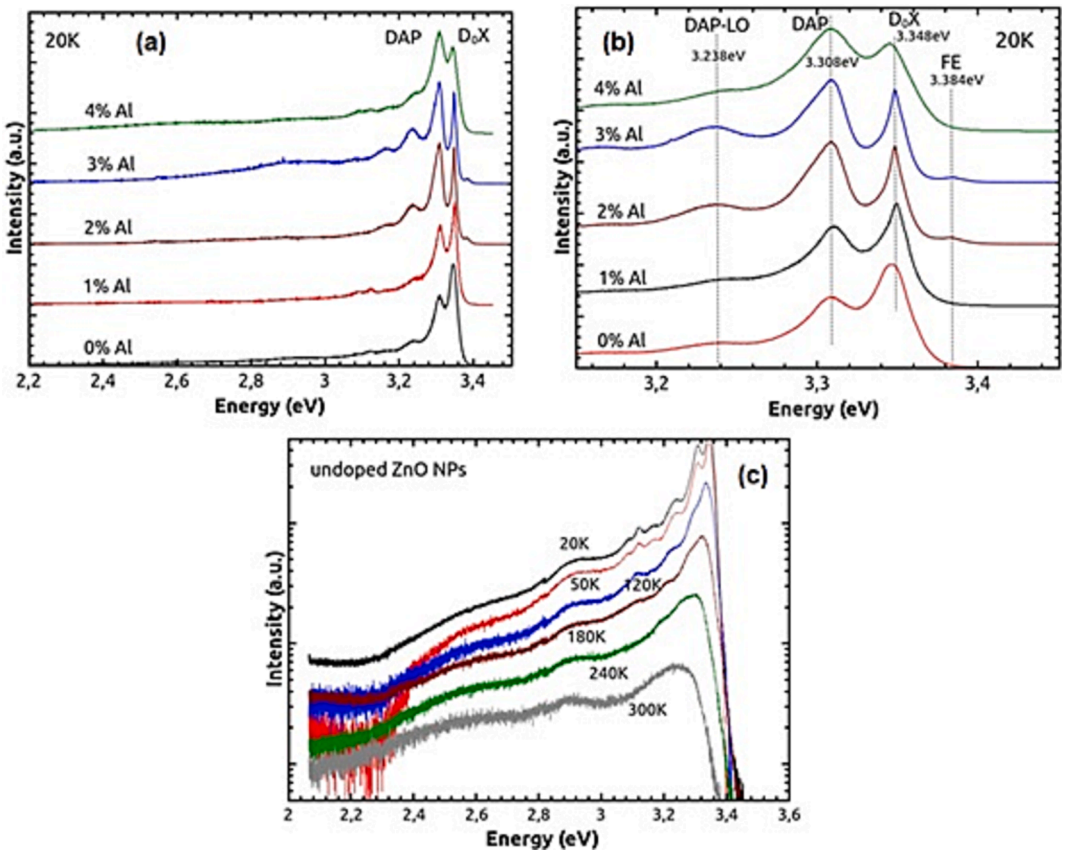

Fig. 4. Photoluminescence patterns of AZO nanoparticles at 20 K: (a) large scan, (b) Near band edge scan and (c) at various temperature for pure ZnO.

Funding

This work was supported by the french national research agency ANR-10-LABX-0022.

CRediT authorship contribution statement

A. Moussa Tankari: Conceptualization, Methodology, Writing – original draft. **K. Medjnoun:** Formal analysis, Data curation, Methodology, Investigation. **M. Nouiri:** Methodology, Validation. **O. Briot:** Investigation, Software. **S. Juillaguet:** Methodology, Investigation. **H. Peyre:** Conceptualization, Methodology. **M. Belaqziz:** Methodology, Formal analysis. **K. Djessas:** Writing – review & editing, Supervision, Project administration, Funding acquisition.

Declaration of Competing Interest

The authors declare that they have no known competing financial interests or personal relationships that could have appeared to influence the work reported in this paper.

Data availability

Data will be made available on request.

References

[1] R.J. Barnes, et al., J. Nanoparticle Res. 15 (2013) 1432.
[2] Z. Zhu, D. Yang, H. Liu, Adv. Powder Technol. 22 (2011) 493–497.
[3] M. Ghaffari, et al., Ceram. Int. 45 (2019) 1179–1188.
[4] A.K. Singh, Adv. Powder Technol. 21 (2010) 609–613.
[5] N. Fathima, et al., Sol. Energy Mater. Sol. Cells 194 (2019) 207–214.
[6] N. Saito, et al., Adv. Mater. 14 (2002) 418–421.
[7] F. Khaled, et al., Vacuum 120 (2015) 14–18.
[8] C. Klingshirn, Phys. Status Solidi B 71 (1975) 547–556.
[9] M. Zareie, et al., Mater. Lett. 91 (2013) 255–257.
[10] M. Farhadi-Khouzani, et al., J. Sol-Gel Sci. Technol. 64 (2012) 193–199.
[11] A. Moulahi, F. Sediri, Ceram. Int. 40 (2014) 943–950.
[12] F.H. Chung, J. Appl. Cryst. 7 (1974) 519–525.
[13] B.D. Cullity, Addison-Wesley Publishing, 1956.
[14] L. Lutterotti, et al., Thin Solid Films 450 (2004) 34–41.
[15] K. Medjnoun, et al., Superlattice. Microst. 82 (2015) 384–398.
[16] S. Hamrit, et al., Ceram. Int. 42 (2014) 16212–16219.
[17] B. Sathya, et al., J. Mater. Sci. Mater. Electron. 28 (2017) 6022–6032.
[18] G. Callsen, et al., Appl. Phys. Lett. 98 (2011), 061906.
[19] H.-G. Park, et al., Bull. Kor. Chem. Soc. 34 (2013) 3335–3339.